Fluorescent Probe Solubilization in the Headgroup and Core Regions of Micelles: Fluorescence Lifetime and Orientational Relaxation Measurements

Stephan Matzinger, Deborah M. Hussey, and M. D. Fayer*

Department of Chemistry, Stanford University, Stanford, California 94305

Received: April 15, 1998; In Final Form: June 26, 1998

Experimental results demonstrate that the fluorescent probes 2-(*N*-hexadecylamino)-naphthalene-6-sulfonate (HANS) and 2-(*N*-decylamino)-naphthalene-6-sulfonate (DANS) are solubilized in two distinct regions, that is, the headgroup and core, within micelles of cetyltrimethylammoniumbromide (CTAB), tetradecyltrimethylammoniumbromide (TTAB), dodecyltrimethylammoniumbromide (DTAB), cetyltrimethylammoniumchloride (CTAC), and tetradecyltrimethylammoniumchloride (TTAC). The fluorescence lifetime decays for both chromophores are biexponential in all the different micelles. The population associated with the shorter lifetime ($\tau_1 \cong 4-5$ ns) is located in the Stern layer, where reduction of the fluorescence lifetime occurs because of quenching induced by the bromide counterions. The second population of chromophores is located in the hydrocarbon core region of the micelle. In this environment the chromophores have a considerably longer lifetime ($\tau_2 \cong 19-20$ ns) because there is no significant quenching by bromide counterions. Evidence of water penetration places them fairly close to the core−Stern layer interface. Time-dependent fluorescence anisotropy is analyzed in terms of these two populations. The measurements show that the orientational relaxation of the probes in the hydrocarbon core region is considerably slower than orientational relaxation in the Stern layer. When the lifetime measurements and the orientational relaxation measurements are combined, the partitioning of the chromophores in the core and headgroup regions of the micelles can be determined.

I. Introduction

In this paper experiments on and analysis of the fluorescence lifetimes and the orientational relaxation of two fluorescent probes, 2-(*N*-hexadecylamino)-naphthalene-6-sulfonate (HANS) and 2-(*N*-decylamino)-naphthalene-6-sulfonate (DANS), in five micelles, cetyltrimethylammoniumbromide (CTAB), tetradecyltrimethylammoniumbromide (TTAB), dodecyltrimethylammoniumbromide (DTAB), cetyltrimethylammoniumchloride (CTAC), and tetradecyltrimethylammoniumchloride (TTAC), are reported. Careful analysis of the data and comparison of the micelle data with data taken in a variety of homogeneous solvents of varying concentrations of micelle counterions reveals a remarkable feature of these systems. While the majority of the HANS and DANS chromophores are located in the headgroup region (Stern layer) of the micelles, a detectable amount of the probes dissolves in the hydrocarbon core. The location of the probes in the two regions is evidenced by differences in lifetimes and orientational relaxation times. The fraction of the probe chromophores that reside in each region can be determined by analyzing the time-dependent data.

The use of fluorescent probes has become a widespread approach for investigating properties of micelles, vesicles, and membranes.[1−8] Various types of fluorescence experiments have been employed to study these systems, but steady-state fluorescence spectroscopy remains the most widely used technique. For a method based on the use of fluorescent probes to be applied successfully, the fluorescent molecule must be tailored to probe the desired environment within the microheterogeneous medium under investigation. To ascertain that the probe is located in the target environment, various probe properties, like the positions and shapes of the absorption and fluorescence bands, can be compared to those in bulk-phase systems that mimic the conditions in the microenvironments. The choice of these comparative systems is not always straightforward, since the conditions in bulk-phase analogues of the environments in the microheterogeneous system can actually be quite different from the latter system.[9] This is true in particular for the hydrocarbon core of a micelle. It is often mimicked with hydrocarbon solvents, thus neglecting the notable water content of the regions close to the interface layer, where water penetration can be significant. Because the fluorescence properties of many probes are quite sensitive to the presence of water, especially if there is hydrogen bonding, it becomes necessary to understand the behavior of the probe in considerable detail before an unequivocal interpretation of the experimental results can be made.

When a chromophore is dissolved in the Stern layer of an ionic micelle, the local environment is very complex due to the presence of charged headgroups and counterions in an aqueous solution of limited spatial extent. The high ionic strength (salt concentration equivalent to ~3 M[10]) and the presence of electric fields in the interface region make it difficult to find a well-defined model system in which to study the fluorescence behavior of the probe prior to its application.[11] Despite these considerations, fluorescent chromophores have been successfully used to probe microheterogeneous environments. Time-resolved techniques, such as time-resolved fluorescence lifetime and depolarization measurements, can add a wealth of information on a particular system, thus overcoming some of the limitations mentioned before.

* Corresponding author.

S1089-5647(98)01860-4 CCC: $15.00
Published on Web 08/20/1998

SCHEME 1

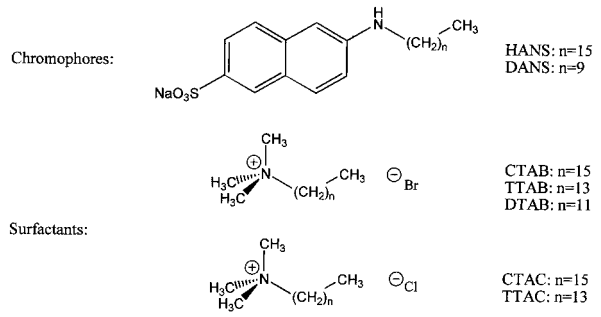

As a result of the amphiphilic nature of surfactant molecules, the difference in the properties of the microheterogeneous environments they form is usually quite distinct. It is therefore not surprising that most probes prefer a specific solubilization site within such a system, depending on the nature of the particular probe molecule. However, the application of time-resolved fluorescence techniques clearly demonstrates that for the probe/micelle systems studied here, the probe is in fact solubilized in two distinct regions of the micelles. To our knowledge this is the first report of such dual solubilization.

The remainder of this paper is organized as follows. In section II, the materials and experimental setup are described. In section III, the time-dependent fluorescence lifetime and depolarization experimental results are presented and analyzed, and in section IV some concluding remarks are made.

II Experimental Procedures

A. Materials. 2-(*N*-Hexadecylamino)-naphthalene-6-sulfonate (HANS) and 2(*N*-decylamino)-naphthalene-6-sulfonate (DANS) (both as the respective sodium salts) were purchased from Molecular Probes Inc., Eugene, OR, and checked for purity by TLC using a series of eluents of different polarity. Cetyltrimethylammoniumbromide (CTAB), cetyltrimethylammoniumchloride (CTAC), tetradecyltrimethylammoniumchloride (TTAC), and tetramethylammoinumbromide (TMAB) were obtained from Fluka. Tetradecyltrimethylammoniumbromide (TTAB) and dodecyltrimethylammoniumbromide (DTAB) were obtained from Aldrich Chemicals, Milwaukee, MI (see Scheme 1). All compounds were purchased in the highest available grade and checked for fluorescent impurities but otherwise used as received from the manufacturer. 2-Aminonaphthalene-6-sulfonic acid was obtained from TCI America Corp. Aqueous solutions of 2-aminonaphthalene-6-sulfonate (ANS) were obtained by neutralizing the acid with an equimolar amount of NaOH.

The chromophore concentration in micellar solutions was 1×10^{-4} M. To guarantee a low probability of having two or more chromophores occupy a single micelle, the micelle concentration, [M], was 10 times higher than the chromophore concentration (1×10^{-3} M). For Poissonian chromophore occupation statistics, this ensures that less than 5% of the occupied micelles carry two or more chromophores, effectively preventing electronic excitation transport among the chromophores. The micelle concentration is a function of the surfactant concentration, [S], the aggregation number, N_{agg}, and the critical micelle concentration, cmc, as follows:

$$[M] = ([S] - cmc)/N_{agg} \quad (1)$$

The values used for these quantities are listed in Table 1. Because the fluorescence spectrum of ANS chromophores depends on the pH, the pH of all solutions was measured to ensure a value between 7 and 8.

TABLE 1: Micelle Properties

micelle	cmc[a] (in mM)	N_{agg}[a]	[S] (in mM)	r_m (in Å)[b]	τ_m (in ns)[c]
CTAB	0.955	92	93.0	35.5	44.7
CTAC	1.3	90	91.3	27.2	20.1
TTAB	3.5	68	71.5	27.9	21.6
TTAC	5.4[d]	65[d]	70.4	24.5	14.6
DTAB	15.4	54	69.4	24.1	14.1

B. Instruments. UV−vis spectra were recorded with a Varian Cary-13e spectrometer, and steady-state fluorescence spectra were measured using a Perkin-Elmer LS-50B fluorescence spectrometer. Fluorescence lifetime and fluorescence depolarization decays were measured using a time-correlated single photon counting system. The excitation pulse from a cavity-dumped and synchronously pumped dye laser (dye: LDS 698 from Exciton Chemical Co.) was frequency doubled and tuned to 355 nm. The details of the apparatus[12] and the technique have been previously described.[13] Briefly, the laser pulse repetition rate was 823 kHz. The fluorescence was collected from the front face of the sample and passed through a subtractive double monochromator to a Hamamatsu microchannel plate detector. The instrument response function was ~50 ps fwhm. For the fluorescence lifetime measurements, the polarization of the excitation beam was set at 54.7° (magic angle) respective to the polarizer in front of the detector. For the measurement of fluorescence depolarization decays, the excitation beam was rotated with a Pockels cell while the detector polarizer was held fixed. Decays parallel ($I_{||}$) and perpendicular ($I_{\perp}$) to the polarization of the excitation beam were collected in an alternating manner under computer control for equal amounts of time (changing every 20 s) until at least 20 000 fluorescence counts were registered in the peak channel of $I_{||}$. The time-dependent fluorescence anisotropy, $r(t)$, was calculated from these data by using the equation

$$r(t) = (I_{||} - I_{\perp})/(I_{||} + 2I_{\perp}) \quad (2)$$

All measurements were carried out at room temperature (stabilized at 24.6 ± 0.5 °C).

III. Results

A. Lifetime Measurements. Figure 1 displays typical fluorescence lifetime decay data for the HANS chromophore dissolved in CTAB solution using a wide detection bandwidth centered around 410 nm. This setting of the monochromator allows detection of photons emitted over the entire fluorescence band. The data in Figure 1 are displayed on a log plot over 5 decades of decay. The decay is clearly nonexponential in contrast to the single-exponential fluorescence decay characteristic of a homogeneous solution. Analysis of the decay curve showed that it could be fit successfully with a biexponential decay function of the form

$$F(t) = A_1 \exp\left(\frac{-t}{\tau_1}\right) + A_2 \exp\left(\frac{-t}{\tau_2}\right) \qquad A = A_1/A_2 \quad (3)$$

with a fast lifetime component $\tau_1 = 4.0$ ns, a second component $\tau_2 = 19.1$ ns, and a ratio, A, of the preexponential factors of 9.1. The data analysis was carried out following the concepts laid out by Grinvald and Steinberg[14] and others.[15,16] A program based on the Levenberg−Marquardt algorithm[17,18] was developed to fit the experimental data to eq 3 convolved with the instrument response. The instrument response function, mea-

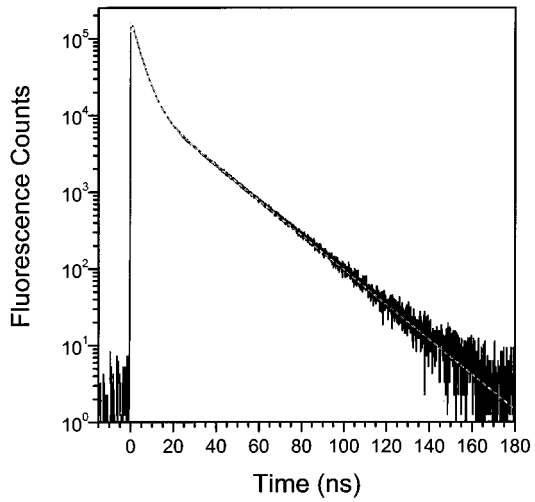

Figure 1. Time-dependent fluorescence decay data of a 10^{-4} M solution of HANS in CTAB (chromophore concentration/micelle concentration = [HANS]/[M] = 1:10) (black line) and corresponding fit to a biexponential decay function (gray line). The parameters for the biexponential decay are $A = 9.1$, $\tau_1 = 4.0$ ns, and $\tau_2 = 19.1$ ns (for an explanation of the parameters see text).

sured using a scatterer, was fit to a sum of three Gaussians so that fast analytical convolutions could be used during the fitting procedure. The quality of the fit was evaluated by inspection of the residuals, the autocorrelation function of the residuals, and the value of the reduced χ^2 ratio. A rigorous error analysis on the parameters obtained from the convolved biexponential fits to the fluorescence data is difficult to accomplish. We estimate an error of 5% on the lifetime and the ratio of the preexponential factors from the range of values obtained from several repeated experiments and from visual inspection of the fits. In no case was the quality of the fit significantly improved by using tri-exponential or higher multiexponential fitting functions, thus validating the choice of a biexponential function. A very similar fluorescence decay is also measured for the DANS chromophore in CTAB solution. For DANS, the measured fluorescence curve can be fit with $A = 8.7$, $\tau_1 = 5.0$ ns, and $\tau_2 = 19.3$ ns.

A possible explanation for the biexponential decay is a partitioning of the chromophores between the micellar environment and the surrounding aqueous solution, leading to two distinct populations with different fluorescence lifetimes. An observation of partitioning between a micelle and water has been made for naphthalene in CTAB solution by Hautala et al.[1] In their experiments, the fluorescence lifetime of one component matched the lifetime of naphthalene in water, supporting the proposition that the chromophores partition between the micelles and the surrounding water. For the probe/micelle systems studied in this work, this explanation is incorrect because HANS does not dissolve in pure water. DANS has a low solubility in water, and the fluorescence lifetime of DANS in water is ~13.5 ns, matching neither the short nor the long lifetime component of the DANS decay in the CTAB micelles. Furthermore, the fluorescence depolarization decay of DANS in water is very fast, $\tau_r = 77$ ps (τ_r is the orientational relaxation decay time), and on the same order as the instrument response. The fastest component of the anisotropy decay of DANS in CTAB is at least a factor of 4−5 larger (see below). The biexponential decays are not due to a partitioning of the probes between the micelles and water.

Substituted aminonaphthalenesulfonate (ANS) chromophores have been widely used as fluorescent probes in proteins and membranes[19,20] due to the large variations in their fluorescence properties in environments of different polarity. For example, these chromophores exhibit strong fluorescence in apolar environments but weak fluorescence in water. The large shifts in the peak wavelength of the fluorescence emission in different solvents can be explained in terms of a large difference between the dipole moment of the chromophore in the ground state (μ_g) and the first excited state (μ_e). Seliskar and Brand have extensively characterized a series of ANS chromophores[21,22] and reported the value for the difference of the dipole moments between the ground and first excited electronic states ($\mu_e - \mu_g$) obtained by an analysis of the solvent-dependence of the steady-state fluorescence energies. They measured a value of 9 D for $\mu_e - \mu_g$ for the parent 2-aminonaphthalene-6-sulfonate and an even larger difference of 23 D for the monosubstituted *N*-cyclohexyl-2-aminonaphthalene-6-sulfonate. Although the authors warn of errors on the absolute values of as much as 50%, it is nevertheless evident that in these molecules the first excited state is much more polar than the ground state. Large differences in the dipole moments of the ground and first excited states cause a red shift in the position of the steady-state fluorescence band in polar solvents compared to nonpolar ones. Furthermore, the time-dependent fluorescence of the chromophore is affected as the solvent reorganizes around the excited chromophore. In recent years, several groups have studied the time-resolved solvation of similar chromophores.[20,23,24] Dependent on the viscosity of the environment, the time scales on which these time-dependent solvent relaxation processes take place are on the order of a picosecond to several nanoseconds.[20,25,26]

Since the micellar environment is often characterized as fairly viscous, it would not be impossible for the decay curves for the HANS/CTAB system to show signs of solvent relaxation processes on the nanosecond time scale. However, due to the large bandwidth of the monochromator used in the previous set of experiments, signs of a time-dependent spectral shift would be difficult to resolve. Therefore, experiments were conducted using a 5 mm slit to limit the monochromator bandwidth to a fwhm of ~14 nm. Fluorescence lifetime decays were then measured by tuning the monochromator to different wavelengths from 375 to 510 nm. With this series of decay curves, $D(t,\lambda)$, it was then possible to reconstruct the fluorescence spectrum, $S(\lambda,t)$, for a desired time t after the excitation pulse. This was done following the method of Maroncelli et al.[27] by relative normalization of the different wavelengths using the steady-state fluorescence spectrum, $S_0(\lambda)$, as follows:

$$S(t) = D(t, \lambda)\frac{S_0(\lambda)}{\int_0^\infty D(t, \lambda)\, \mathrm{d}t} \tag{4}$$

The steady-state spectrum was recorded at 1 nm resolution, convolved with a 14 nm fwhm Gaussian, and fitted to a log-normal curve[28] in order to approximate the steady-state spectrum as measured by our time correlated single photon counting system. The log-normal curve had the following form[27]

$$g(\nu) = g_0 \exp\left\{-\ln 2\left[\frac{\ln\left(1 + 2b\,(\nu - \nu_p)/\Delta\right)}{b}\right]^2\right\} \qquad 2b(\nu - \nu_p)/\Delta > -1 \tag{5}$$

where g_0 is the peak height (=1 in the normalized spectrum), b the peak asymmetry (−0.170), ν_p the peak frequency at the maximum (24 016 cm^{-1}), and Δ the peak width (3160 cm^{-1}), which is related to the fwhm, Γ, by $\Gamma = \Delta(\sinh(b)/b)$.

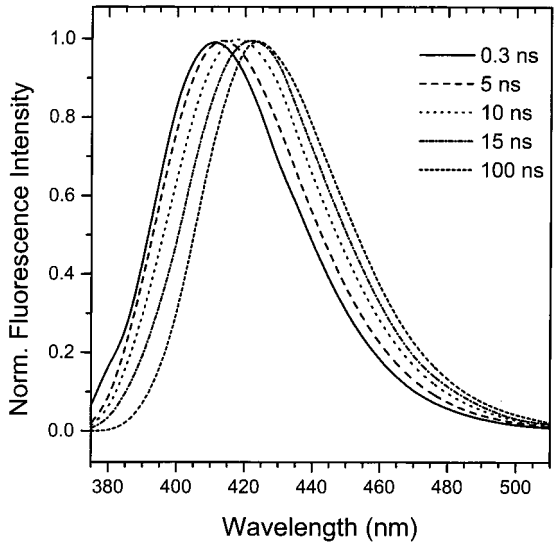

Figure 2. Time-dependent fluorescence spectrum of a 10^{-4} M solution of HANS in CTAB (chromophore concentration/micelle concentration = [HANS]/[M] = 1:10) shown 0.3, 5, 10, 15, and 100 ns after excitation by the laser pulse. See text for details.

Nonlinear least-squares fits to the decay data using the function given in eq 3 were used for $D(t, \lambda)$ instead of the actual data sets, permitting the calculation of the integral in the denominator of eq 4 analytically and circumventing problems due to a low signal-to-noise ratio at very long times. The result of this procedure is the series of fluorescence spectra in time as depicted in Figure 2. At $t = 0$ the fluorescence spectrum peaks at 411 nm, then shifts toward the red, reaching an endpoint at 424 nm, 100 ns after the excitation pulse. A red shift of only 13 nm due to solvent relaxation is atypical for an ANS chromophore, and the time scale is very long.

Furthermore, the fact that each individual decay curve $D(t,\lambda)$ could be fit to a decaying biexponential function rules out a time-dependent solvent relaxation phenomenon as a cause for the 13 nm spectral shift. If solvent relaxation is responsible for a nonexponential decay, it has different characteristics when monitoring the blue and red portions of the spectrum. The spectrum shifts from blue to red. If a blue portion of the spectrum is monitored, the spectrum shifts partially out of the window that is being observed. This produces a fast decay component at a rate associated with the rate of solvent relaxation. At long time, once solvent relaxation is complete, the fluorescence lifetime is observed. If a red portion of the spectrum is monitored, the spectrum shifts partially into the window that is being observed. This produces a buildup of the fluorescence at a rate determined by the rate of solvent relaxation, followed by a decay with the fluorescence lifetime at long time. Therefore, if solvent relaxation caused the time-dependent spectral shift, at the detection wavelengths far to the red an initial buildup of fluorescence intensity should be observable. Since a buildup with a time scale the same as the faster component of the decay shown in Figure 1 was not observed when the red edge of the fluorescence band was monitored, time-dependent solvent relaxation does not significantly affect the data, at least not at times longer than ~2 ns. Small deviations from the convolved fits to a biexponential decay at times less than 2 ns were observed in the wavelength-resolved experiments. These might be caused by fast solvent relaxation but were not analyzed in further detail.

The analysis presented above rules out solvent relaxation and partitioning of the probes between the micelle and water as causes of the observed biexponential decays of HANS and DANS in CTAB micelles. A third possibility is that the probe chromophores are partitioned between two distinct environments within the micelles. The two microenvironments, the headgroup and core regions of the micelles, have quite different properties. While the inside of the micelle is usually characterized as a viscous, apolar, and hydrocarbon-like liquid, the headgroup interface layer (Stern layer) has a large concentration of ionic headgroups and counterions in a partially aqueous medium with dramatically different properties from the interior of the micelle. Normally it would not be assumed that the chromophore could be present in both microenvironments at the same time. If the chromophore is in a single region, then a single-exponential decay would be expected. Nevertheless, the results presented below provide compelling evidence supporting the fact that while the chromophores are mainly located in the headgroup region, a non-negligible fraction (~10%) of the chromophores is located in the core. To our knowledge, no such system has been reported previously. The chromophores, located in the core near the core−Stern layer boundary, give rise to the slow component of the decay in Figure 1, and the chromophores located in the Stern layer give rise to the fast component of the decay.

While it is well established that the bromide counterion in CTAB micelles can quench the fluorescence of aromatic chromophores,[1,29−32] the nature of the quenching mechanism is still a matter of debate and probably depends on the chromophore. Two possible mechanisms for the quenching process have been proposed, namely, quenching by the external heavy-atom effect[30,31] and quenching by electron transfer (charge-transfer complexes).[33−35] It is also known that the chloride counterion in CTAC does not significantly quench the fluorescence of these compounds. To determine the influence of the bromide counterion on our system, we therefore replaced the CTAB surfactant by CTAC, which differs only in the counterion. Again, a biexponential fluorescence decay is observed. The nonlinear least-squares fit yielded values of $A = 8.2$, $\tau_1 = 9.4$ ns, and $\tau_2 = 19.9$ ns for the HANS/CTAC system and $A = 7.8$, $\tau_1 = 9.6$ ns, and $\tau_2 = 19.6$ ns for the DANS/CTAC system. Compared to data from the same chromophores in CTAB, τ_1 is longer by a factor of ~2 while τ_2 is virtually unchanged. Both the external heavy-atom effect and electron-transfer mechanisms act at short range, and it is therefore necessary for the chromophore and the counterion to diffuse together for quenching to occur. It can therefore be concluded that in a CTAB solution, the population of chromophores with the shorter lifetime, τ_1, is in close proximity to the bromide ions, as indicated by the change in fluorescence lifetime upon exchange of the counterion.

Experiments on the parent ANS chromophore in different salt solutions provide further information on the nature of the fluorescence quenching. In a series of 1 M solutions of KCl, KBr, and KI, the fluorescence lifetime is a single exponential. Figure 3 shows decays from the three solutions along with single-exponential fits to each data set. The observed lifetimes are 14.3, 11.3, and 2.3 ns in the three solutions compared to 14.1 ns in pure water. In 1 M tetramethylammoniumbromide (TMAB), a salt very similar to CTAB except without the long hydrocarbon tail, 11.2 ns was measured for the ANS fluorescence lifetime. This value is basically identical to the one obtained in the KBr solution. One can therefore conclude that the anion is responsible for the observed quenching process. The quenching rate increases in the series from the chloride

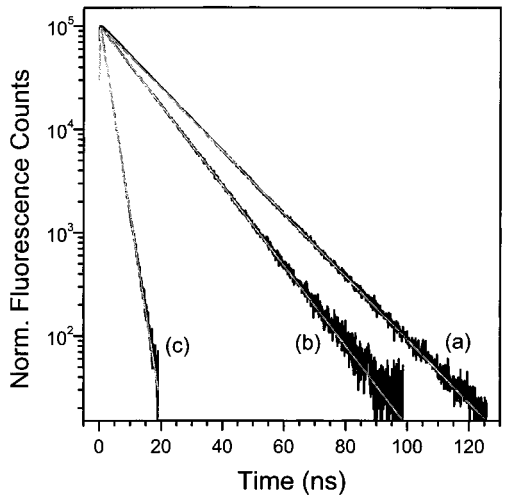

Figure 3. Time-dependent fluorescence decay data of a 5×10^{-4} M solution of ANS in a 1 M solution of KCl (a), in 1 M KBr (b), and in 1 M KI (c) (black lines). Corresponding fits to a single-exponential decay function are plotted as the gray lines. The lifetimes are (a) 14.3 ns, (b) 11.3 ns, and (c) 2.3 ns.

ion, to the bromide ion, to the iodide ion, with the chloride ion having little effect. These results are consistent with the external heavy-atom effect or an electron-transfer mechanism. In either case, the interaction responsible for the effect is a very short-range exchange interaction, and therefore, the anion must be in close proximity to the chromophore to induce fluorescence quenching.

A fluorescence lifetime of 7.9 ns was measured in a saturated (~3.6 M) TMAB solution. The actual concentration of bromide ions in the Stern layer of CTAB has been estimated to be ~3 M.[10] The lifetime measured in the saturated TMAB solution is in agreement with the measurement of the CTAB micelles if we consider that in micelles, the lifetime is already lower in the absence of bromide ions (in CTAC) than in water. The bromide concentration in the intermicellar water region is very low.[36] Therefore, for the observed fluorescence lifetime to be so short in the micellar solution, the excited chromophore has to be in close proximity to the high local bromide concentration in the Stern layer. The lifetime τ_1 is also reduced by a factor of 2 by the presence of bromide counterions compared to the chloride ions, which further substantiates this conclusion.

As can be seen from the lifetime data presented above, the second population of chromophores (with lifetime τ_2) is nearly unaffected by the exchange of the bromide for chloride ions. This indicates that the chromophore is in a microenvironment where it cannot be reached by these ions. The second population is not in the surrounding water phase for the reasons outlined at the beginning of this section. The micelle interior is the region where the chromophores cannot be reached by bromide ions. Although some authors suggested the possibility that a low concentration of bromide ions can reach the interior of the micelle via water channels penetrating into the hydrocarbon core,[29,37−41] such penetration would not result in the high bromide concentration necessary to produce a significant decrease in the fluorescence lifetime.

In the partitioning model, where the same type of chromophore is present in two distinct regions of the micelle, we can calculate the fraction of chromophores in each environment if we assume that the extinction coefficient of the chromophore in the two environments at the excitation wavelength is the same. This is a reasonable approximation. The chromophore is not very polar in its ground state. The absorption spectrum is approximately the same in polar and nonpolar media. Then, the total fluorescence intensity, I, emitted from the sample can be calculated by integrating the biexponential fluorescence decay function (eq 3) over time:

$$I = \int_0^\infty F(t)\,\mathrm{d}t = \tau_1 A_1 + \tau_2 A_2 = I_1 + I_2 \tag{6}$$

To obtain the partitioning coefficient, the measured intensities for the two components I_1 and I_2 have to be weighted by the quantum yields (Φ_1 and Φ_2) to correct for differences in the nonradiative decay processes in the two environments:

$$I_1^c = \frac{\tau_1 A_1}{\Phi_1} \quad I_2^c = \frac{\tau_2 A_2}{\Phi_2} \tag{7}$$

Then the partitioning coefficient, P, is obtained by

$$P = \frac{I_1^c}{I_2^c} = \frac{\tau_1 A_1}{\tau_2 A_2}\frac{\Phi_2}{\Phi_1} = \frac{\tau_1 A_1}{\tau_2 A_2}\frac{\tau_2}{\tau_1} = \frac{A_1}{A_2} = A \tag{8}$$

because the quantum yields can be expressed as the quotient of the measured lifetime over natural lifetime (lifetime in the absence of nonradiative processes).[42,43] A value of 9.1 was obtained for A in the biexponential fit of the fluorescence decay of the HANS/CTAB system. We can now interpret this value as an estimate for the partitioning of the HANS chromophore into the two solubilization regions. About 9 times as many chromophores are located in the Stern layer as in the core of the micelle. A very similar partitioning is found for DANS in CTAB with $A = 8.7$. The affinity for the Stern layer seems to be slightly reduced in the CTAC micelles, where partition coefficients of $A = 8.2$ and $A = 7.8$ were found for the HANS and DANS chromophores, respectively.

In consideration of the time-dependent spectral shifts discussed above, the apparent shift is due to the faster decay of the Stern layer chromophore population, leaving more of the slow micelle core component behind at long times. The spectral shift to the red as time increases arises because the fluorescence spectrum of the chromophores in the inside of the micelle is red-shifted compared to that of the chromophores in the Stern layer. A chromophore's fluorescence in a homogeneous apolar environment is normally blue-shifted compared to its fluorescence in a more polar solvent. This is also the case for ANS-type chromophores.[22,44−46] However, high ionic strength and the presence of an electric field in the Stern layer are both believed to shift the fluorescence of the chromophores in the Stern layer,[11,9] possibly to the blue, leading to an apparent anomalous red shift between the two components. Another possible factor contributing to the blue shift of the Stern layer chromophores is hydrogen bonding between the chromophores and water molecules in the Stern layer. As a result of spatial constraints, the chromophore/water hydrogen bonds in the Stern layer may be different from those formed in bulk water,[9] thus further affecting the position of the fluorescence emission.[47] Other specific surfactant/chromophore interactions have been proposed for aromatic sulfonates,[48,49] possibly further shifting the emission band position.

B. Orientational Relaxation. In addition to the information presented above on fluorescence quenching by bromide counterions, analysis of fluorescence depolarization data gives further insights into the solubilization of the probe chromophores, HANS and DANS, into two regions, the headgroup and core of the micelles. It is impossible to fit the fluorescence depolarization data acquired for HANS in CTAB satisfactorily

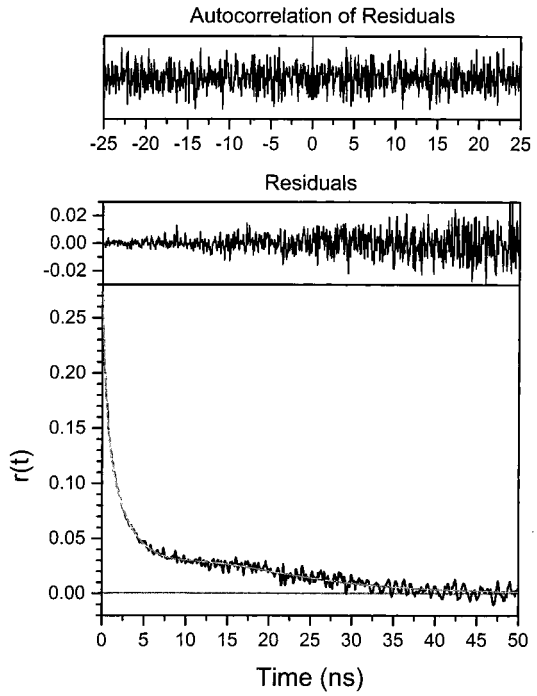

Figure 4. Time-dependent fluorescence anisotropy decay data obtained in the measurement of a sample of a 10^{-4} M solution of HANS in CTAB (chromophore concentration/micelle concentration = [HANS]/[M] = 1:10) (black line) and the fitting function to these data (in gray). The fit was obtained for a two-component mixture. The first component is modeled as a biexponential anisotropy decay with $r_1^{(1)} = 0.12$, $\tau_{r1}^{(1)} = 0.48$ ns, $r_2^{(1)} = 0.16$, and $\tau_{r2}^{(1)} = 2.9$ ns. The second component is modeled as a single-exponential decay with $r^{(2)} = 0.16$ and $\tau_r^{(2)} = 10.7$ ns. The fraction of component 1 was $f_1 = 0.9$, as obtained from the fit of the time-dependent fluorescence spectrum. The residuals of the fit and the autocorrelation of the residuals are shown as a diagnostic for the quality of the fit in the upper part of the plot. See text for explanation of parameters.

with a multiexponential decay function. As can be seen in Figure 4, the decay curve flattens between ~10 and 20 ns and then decreases more rapidly again. At first glance this might look like an artifact. However, the theoretical functional form of the anisotropy decay, $r(t)$, for a fluorescent probe partitioned between two microenvironments is not straightforward, as chromophores in different environments may have distinct fluorescence lifetime and anisotropy properties. Lentz et al.[2] have previously worked out formulas for $r(t)$ in a multicomponent system. Here, the problem will be treated in a slightly different and more general form.

For a macroscopically homogeneous and isotropic sample, the fluorescence intensity in the parallel ($I_{||}$) and perpendicular ($I_\perp$) directions as measured in the experiments is composed of the following contributions in a two-component system:

$$I_{||}(t) = f_1 I_{||}^{(1)}(t) + f_2 I_{||}^{(2)}(t)$$

$$I_\perp(t) = f_1 I_\perp^{(1)}(t) + f_2 I_\perp^{(2)}(t) \qquad (9)$$

f_1 and f_2 are the fractions of photons emitted by fluorescence from components 1 and 2, respectively ($f_1 + f_2 = 1$) and are linked to the pre-exponential factors A_1 and A_2 in the biexponential fluorescence decay (see eq 3). $I_{||}^{(k)}(t)$ and $I_\perp^{(k)}(t)$ are the time-dependent parallel and perpendicular intensities of the two components, k, that would be measured in our experiment if all the probes were uniquely in environment k. Starting the derivation from eq 2, the following expression is obtained:

$$r(t) = \frac{I_{||}(t) - I_\perp(t)}{F(t)} = \frac{f_1(I_{||}^{(1)}(t) - I_\perp^{(1)}(t)) + f_2(I_{||}^{(2)}(t) - I_\perp^{(2)}(t))}{f_1(I_{||}^{(1)}(t) + 2I_\perp^{(1)}(t)) + f_2(I_{||}^{(2)}(t) + 2I_\perp^{(2)}(t))} \qquad (10)$$

where $F(t) = I_{||}(t) + 2I_\perp(t)$ is the total fluorescence decay; see, for example Figure 1. This can be further simplified into

$$r(t) = \frac{f_1\frac{F_1(t)}{F_1(t)}(I_{||}^{(1)}(t) - I_\perp^{(1)}(t)) + f_2\frac{F_2(t)}{F_2(t)}(I_{||}^{(2)}(t) - I_\perp^{(2)}(t))}{f_1F_1(t) + f_2F_2(t)}$$

$$r(t) = \frac{1}{F(t)}[f_1F_1(t)r_1(t) + f_2F_2(t)r_2(t)] \qquad (11)$$

where $F_1(t)$ and $F_2(t)$ are the total fluorescence decays and $r_1(t)$ and $r_2(t)$ are the anisotropy decay functions for pure environments 1 and 2, respectively. It is simple to extend this formula to an n-component system where $r(t)$ is given by

$$r(t) = \frac{1}{F(t)}[f_1F_1(t)r_1(t) + f_2F_2(t)r_2(t) + ... + f_nF_n(t)r_n(t)] \qquad (12)$$

It is clear from this result that the observed anisotropy decay for the mixture depends on both components simultaneously. Because each anisotropy constituent is weighted by its own fluorescence decay function, there will be regions of the total anisotropy decay that are more sensitive to one or the other anisotropy component. A fitting procedure implementing this functional form for the total anisotropy decay can take advantage of this and obtain a fit for $r_1(t)$ and $r_2(t)$ simultaneously. A fitting program based on the Levenberg−Marquardt algorithm[17,18] was developed for this purpose. The following two anisotropy decay functions were fit to the data:

$$r_1(t) = r_1^{(1)}\exp(-t/\tau_{r1}^{(1)}) + r_2^{(1)}\exp(-t/\tau_{r2}^{(1)})$$

$$r_2(t) = r^{(2)}\exp(-t/\tau_r^{(2)}) \qquad (13)$$

The anisotropy decay associated with the faster fluorescence decay, $r_1(t)$, is modeled as a biexponential decay function. This is consistent with the wobbling-in-a-cone model for restricted orientational diffusion for a chromophore in the Stern layer of the micelle, which predicts one or two dominant contributions in a multiexponential decay.[50,51] The anisotropy decay of the population in the core region of the micelle, $r_2(t)$, is modeled as a single-exponential decay. No obvious restriction of the motion of the interior chromophore population is apparent. Therefore, it is modeled as an isotropic orientational diffusion process, leading to a single-exponential anisotropy decay.

As a representative example of these fits, Figure 4 depicts the fluorescence depolarization decay of HANS in CTAB as well as the corresponding fit. In addition, the residuals and the autocorrelation of the residuals are shown. Clearly, the functional form and the fit to the data are in excellent agreement with the data. The numerical values of the parameters in eq 13 obtained from fitting the data for all the chromophores and micelles used in this study are listed in Table 3. A rigorous error assessment of the fit parameters is not possible. As a result of the many parameters necessary to describe the anisotropy decays, the errors on the decay constants are larger than those of the lifetimes given in Table 2. The first column in Table

TABLE 2: Fluorescence Decay Analysis

		biexponential decay parameters		
chromophore	micelle/solvent	ratio A_1/A_2	τ_1	τ_2
HANS	CTAB/H_2O	9.1	4.0	19.1
HANS	CTAC/H_2O	8.2	9.4	19.9
HANS	TTAB/H_2O	9.2	4.3	19.3
HANS	TTAC/H_2O	8.7	9.7	19.8
HANS	DTAB/H_2O	10.1	4.8	19.4
DANS	CTAB/H_2O	8.7	5.0	19.3
DANS	CTAC/H_2O	7.8	9.6	19.6
DANS	TTAB/H_2O	7.9	4.8	19.2
DANS	TTAC/H_2O	7.1	9.8	19.5
DANS	DTAB/H_2O	8.3	5.1	19.1

TABLE 3: Anisotropy Decay Analysis

		Stern layer component				core component		
system	ratio f_1/f_2	$r_1^{(1)}$	$\tau_{r1}^{(1)}$	$r_2^{(1)}$	$\tau_{r2}^{(1)}$	$r^{(2)}$	$\tau_r^{(2)}$	τ_{rI}
HANS/CTAB	9.0	0.12	0.48	0.16	2.9	0.16	10.7	14.1
HANS/TTAB	8.1	0.14	0.42	0.15	2.0	0.20	6.3	8.9
HANS/DTAB	10.1	0.15	0.39	0.13	1.7	0.18	4.8	7.3
DANS/CTAB	8.1	0.15	0.61	0.13	3.1	0.12	10.7	14.1
DANS/TTAB	8.1	0.14	0.44	0.13	2.0	0.15	6.0	8.3
DANS/DTAB	9.0	0.13	0.34	0.13	1.3	0.24	3.6	4.8
HANS/CTAC	8.1	0.12	0.40	0.13	1.8	0.29	6.9	10.5
HANS/TTAC	9.0	0.11	0.30	0.15	1.3	0.34	4.8	7.2
DANS/CTAC	7.3	0.16	0.49	0.12	2.6	0.11	10.8	23.3
DANS/TTAC	8.1	0.10	0.29	0.14	1.2	0.32	3.9	5.3

3gives the ratio f_1/f_2. This is the equivalent of the ratio A_1/A_2 in Table 2, but it is obtained from the fluorescence depolarization data. While not identical, the ratios in the two tables are very similar (note the order of presentation of the samples is different in Tables 2 and 3). While the two-component hypothesis is mainly based on the lifetime and fluorescence quenching data presented above, the two-component model is strongly supported by the analysis of the anisotropy data (see below), which has a very distinct shape that would be difficult to obtain using a different model.

Before discussion of the anisotropy decay parameters in further detail, it is necessary to consider the fact that the entire micelle rotates, causing additional orientational relaxation of the chromophores bound to it. Because the micelles are relatively large, their rotational diffusion is slow. Therefore, rotational diffusion of the entire micelle basically affects only the slowest decay component, that is, the population of chromophores in the interior of the micelle with the correlation time $\tau_r^{(2)}$. Because depolarization due to rotational diffusion of the chromophore within the micelle takes place independently of orientational relaxation due to rotation of the entire micelle, the decay rates of these two processes can be added, leading to the following relationship between the correlation times:

$$\frac{1}{\tau_r^{(2)}} = \frac{1}{\tau_{rI}} + \frac{1}{\tau_m} \tag{14}$$

$\tau_r^{(2)}$ is the measured orientational relaxation correlation time; τ_{rI} is the orientational relaxation time of the probe molecule in the micelle interior. τ_m is the correlation time for the micelle orientational relaxation in water, which can be calculated from the Debye−Stokes−Einstein (DSE) equation with "stick" boundary conditions,

$$\tau_m = \frac{4\pi r_m{}^3 \eta}{3k_B T} \tag{15}$$

where r_m is the radius of the micelle, η the shear viscosity of water (0.98 cP), k_B the Boltzmann constant, and T the absolute temperature. Due to uncertainty in the measurement of the micelle radius, r_m, and the use of the DSE equation, τ_m is a source of error in the determination of τ_{rI}. The important point is that the τ_{rI} values are much longer than the $\tau_{r1}^{(1)}$ and $\tau_{r2}^{(1)}$. A correction of the rotational correlation times $\tau_{r1}^{(1)}$ and $\tau_{r2}^{(1)}$ is unnecessary, since they are much shorter than τ_m and the resulting correction is negligible.

Analysis of the fluorescence depolarization decays for the HANS/CTAB and DANS/CTAB systems leads, within the error, to essentially the same decay parameters. For the chromophores in the Stern layer, rotational relaxation is quite fast with $\tau_{r1}^{(1)} = 0.5$ ns and $\tau_{r2}^{(1)} = 3.0$ ns. These values are consistent with those obtained in other studies[5,6] where similar values were found for chromophores in the Stern layer that are anchored in the micelle by hydrocarbon chains. No significant difference in the orientational decay parameters for HANS and DANS is observed. This is not surprising, because the two chromophores differ only in the length of their hydrocarbon tail, which does not participate in the wobbling motion. The second chromophore population in the core region of the micelle experiences a very different environment, in which orientational diffusion is much slower with $\tau_{rI} = \sim 14$ ns. τ_{rI} is considerably longer than the measured decay of DANS in dodecanol ($\sim$4.2 ns), indicating a high local microviscosity at the solubilization site of the probe chromophores in the micelles. The viscosity of dodecanol at 20 °C is 17.4 cP.[52] The microviscosities of the core regions of alkyltrimethylammonium bromide micelles have been found to lie in the range 17−50 cP.[53] The values of τ_{rI} are consistent with the chromophores being located in the hydrocarbon core of the micelle.

So far, data and analysis that have been presented have concentrated on a set of experiments with HANS and DANS in CTAB and CTAC micelles. The results have demonstrated that these chromophores are situated in two distinct solubilization regions within these micelles. These two distinct solubilization regions will each involve a range of slightly different microenvironments that should result in a distribution of lifetimes and orientational relaxation dynamics. However, the microenvironment variations are evidently relatively small and do not lead to detectable spreads in lifetimes and relaxation rates. The characteristics that are measured for the two solubilization sites may actually be averages over a range of values that are similar for each site but vary substantially between the two sites.

To learn more about the behavior of these chromophores in different trimethylalkylammonium micelles, the same set of experiments was repeated with TTAB, TTAC, and DTAB micelles. Generally the results are very similar to the ones already discussed. The fluorescence lifetime of the component located in the core of the micelle was measured to be 19.2 ns for both chromophores in all the micelles with the bromide counterion. The lifetime was only slightly longer in the micelles with the chloride counterion (19.7 ns). Within experimental error, no significant correlation of the lifetime with the size of the micelles was observed. For the chromophores present in the Stern layer, a small trend can be observed only for the HANS chromophore. As the micelles get smaller, a larger fraction of the chromophores partition into the Stern layer as indicated by the increase of A from 9.1 to 10.1 in the series: CTAB, TTAB, DTAB. This trend might be attributed to the decreasing volume of the micellar core, thus favoring a position for the HANS chromophore in the Stern layer. The fluorescence lifetime increases from 4.0 to 4.8 ns in progressing from CTAB to

DTAB. In the micelles with the chloride counterion, a parallel trend can be seen as the lifetime slightly increases from CTAC to TTAC. No systematic trend is, however, detected in this series of micelles with the DANS chromophore. This is most likely because the hydrocarbon chain of DANS is six $-(CH_2)-$ units shorter than that of HANS.

More significant differences are found in the analysis of the anisotropy decays of the various micelles. Considering the series of CTAB, TTAB, and DTAB micelles, it is found that the orientational correlation time of the core component of chromophores, τ_{rI}, decreases from 14 to 7 ns for HANS and from 14 to 5 ns for DANS. It can be assumed that because of the increased curvature of smaller micelles, the penetration of water through channels into the micellar core increases significantly with decreasing micelle size.[29,37−41] The increased water content in the core could lead to sizable changes in the local microviscosity and therefore to the observed decrease in τ_{rI}. A similar decrease of the two Stern layer orientational correlation times $\tau_{r1}^{(1)}$ and $\tau_{r2}^{(1)}$ is observed (see Table 3). An explanation for this trend may be that the degree of order decreases with decreasing micelle radius. Hence, orientational relaxation processes can take place more easily, leading to shorter correlation times. For the CTAC and TTAC micelles similar conclusions can be drawn. These water channels in the hydrocarbon core are located mostly close to the interface of the hydrocarbon core with the Stern layer. This and the fact that the headgroups of the HANS and DANS chromophores are polar would suggest that the chromophore population in the core remains quite close to the core−Stern layer interface.

IV. Concluding Remarks

Both HANS and DANS chromophores are partitioned into two distinct solubilization regions within CTAB, CTAC, TTAB, TTAC, and DTAB micelles in water. Close to 90% of the chromophores are located in the Stern layer of these micelles. Due to the presence of bromide counterions in the Stern layer of CTAB, TTAB, and DTAB micelles, the fluorescence lifetime is shortened by a factor of ∼2 compared with the lifetimes measured in CTAC and TTAC. Because the two mechanisms for quenching, namely electron transfer and the external heavy-atom effect, are both short-range, this observation demonstrates that these chromophores are located in the Stern layer of the micelles, where the local concentration of bromide counterions is very high.

The measured fluorescence polarization anisotropy decays of the Stern layer chromophores are analyzed as biexponential decays with orientational correlation times $\tau_{r1}^{(1)} = 0.3-0.6$ ns and $\tau_{r2}^{(1)} = 1.3-3.1$ ns, with the particular values depending on the chromophore and the micelle (see Table 3). These times are consistent with the chromophores being located in the Stern layer, since similar values have been found for comparable probe molecules in other studies.[5,6] The remaining ∼10% of the chromophores are located in the hydrocarbon core of the micelles. Their fluorescence lifetimes are significantly longer ($\tau_2 = 19-20$ ns) than that of the first population and are virtually unaffected by a change of the counterion from bromide to chloride. The longer lifetime is consistent with a less polar environment and does not match the lifetime of the chromophore in water. The anisotropy decay associated with the longer lifetime shows very slow orientational relaxation ($\tau_{rI} = 5-14$ ns, depending on the micelle; see Table 3) and is highly dependent on the size of the micelle. This evidence places the second population in the interior, hydrocarbon core region of the micelle.

The fluorescence lifetime and time-dependent fluorescence depolarization experiments on the series of trimethylalkylammonium micelles produced compelling evidence for the proposed model in which the fluorescent probes are located in two distinct regions of the micelles. In addition, the changes in lifetime and orientational relaxation rate with micelle size provide insights into the nature of micelle structure.

Acknowledgment. Support for this work was provided by the Department of Energy, Office of Basic Energy Sciences (Grant DEFG03-84ER13251). S.M. thanks the Swiss National Science Foundation for their financial support for a postdoctoral fellowship. D.M.H. thanks the Soroptimists of the Sierra Pacific region for a Dissertation Year Fellowship.

References

(1) Hautala, R. R.; Schore, N. E.; Turro, N. J. *J. Am. Chem. Soc.* **1973**, *95*, 5508.
(2) Lentz, B. R.; Barenholz, Y.; Thompson, T. E. *Biochemistry* **1976**, *15*, 4529.
(3) Blatt, E.; Ghiggino, K. P.; Sawyer, W. H. *J. Phys. Chem.* **1982**, *86*, 4461.
(4) Varnavsky, O.; Grund, I.; Hauser, M.; Klein, U. K. A. *Chem. Phys. Lett.* **1987**, *141*, 99.
(5) Visser, A. J. W. G.; Vos, K.; Hoek, A. v.; Santema, J. S. *J. Phys. Chem.* **1988**, *92*, 759.
(6) Quitevis, E. L.; Marcus, A. H.; Fayer, M. D. *J. Phys. Chem.* **1993**, *97*, 5762.
(7) Sarpal, R. S.; Dogra, S. K. *Indian J. Chem.* **1993**, *32A*, 754.
(8) Chattopadhyay, A.; Mukherjee, S. *Biochemistry* **1993**, *32*, 3804.
(9) Ramachandran, C.; Pyter, R. A.; Mukerjee, P. *J. Phys. Chem.* **1982**, *86*, 3198.
(10) Mukerjee, P. *J. Phys. Chem.* **1962**, *66*, 943.
(11) Gross, D.; Loew, L. M. *Methods Cell Biol.* **1989**, *30*, 193.
(12) Stein, A. D.; Peterson, K. A.; Fayer, M. D. *J. Chem. Phys.* **1990**, *92*, 5622.
(13) O'Connor, D. V.; Phillips, D. *Time-Correlated Single Photon Counting*; Academic Press: London, 1984.
(14) Grinvald, A.; Steinberg, I. Z. *Anal. Biochem.* **1974**, *59*, 583.
(15) O'Connor, D. V.; Ware, W. R.; Andre, J. C. *J. Phys. Chem.* **1979**, *83*, 1333.
(16) McKinnon, A. E.; Szabo, A. G.; Miller, D. R. *J. Phys. Chem.* **1977**, *81*, 1564.
(17) Marquardt, D. W. *J. Soc. Ind. Appl. Math.* **1963**, *11*, 431.
(18) Press, W. H.; Flannery, B. P.; Teukolsky, S. A.; Vetterling, W. T. *Numerical Recipes in C: the art of scientific computing*, 2nd ed.; Cambridge University: Cambridge, 1992.
(19) Stryer, L. *J. Mol. Biol.* **1965**, *13*, 482.
(20) Brand, L.; Gohlke, J. R. *J. Biol. Chem.* **1971**, *246*, 2317.
(21) Seliskar, C. J.; Brand, L. *J. Am. Chem. Soc.* **1971**, *93*, 5405.
(22) Seliskar, C. J.; Brand, L. *J. Am. Chem. Soc.* **1971**, *93*, 5414.
(23) Chakrabarti, S. K.; Ware, W. R. *J. Chem. Phys.* **1971**, *55*, 5494.
(24) Rosenthal, S. J.; Jimenez, R.; Fleming, G. R.; Kumar, P. V.; Maroncelli, M. *J. Mol. Liq.* **1994**, *60*, 25.
(25) Maroncelli, M. *J. Mol. Liq.* **1993**, *57*, 1.
(26) Barbara, P. F.; Jarzeba, W. *Adv. Photochem.* **1990**, *15*, 1.
(27) Maroncelli, M.; Fleming, G. R. *J. Chem. Phys.* **1987**, *86*, 6221.
(28) Siano, D. B.; Metzler, D. E. *J. Chem. Phys.* **1969**, *51*, 1856.
(29) Burrows, H. D.; Formosinho, S. J.; Paiva, M. F. J. R.; Rasburn, J. *J. Photochem.* **1980**, *12*, 285.
(30) Wolff, T. *Ber. Bunsen-Ges. Phys. Chem.* **1982**, *86*, 1132.
(31) Meling, H.; Wolff, T.; Bünau, G. v. *Ber. Bunsen-Ges. Phys. Chem.* **1988**, *92*, 200.
(32) Sarpal, R. S.; Dogra, S. K. *J. Photochem. Photobiol, A* **1995**, *88*, 147.
(33) Brooks, C. A. G.; Davis, K. M. C. *J. Chem. Soc., Faraday Trans. 2* **1972**, 1649.
(34) Bendig, J.; Siegmund, M.; Helm, S. *Adv. Mol. Relax. Interact. Processes* **1979**, *14*, 121.
(35) Mac, M.; Najbar, J.; Phillips, D.; Smith, T. A. *J. Chem. Soc., Faraday Trans.* **1992**, *88*, 3001.
(36) Cuccovia, I. M.; Da Silva, I. N.; Chaimovich, H.; Romsted, L. S. *Langmuir* **1997**, *13*, 647.
(37) Rodgers, M. A. J.; da Silva e Wheeler, M. E. *Chem. Phys. Lett.* **1976**, *43*, 587.
(38) Rodgers, M. A. J.; da Silva e Wheeler, M. E. *Chem. Phys. Lett.* **1978**, *53*, 165.
(39) Menger, F. M.; Jerkunica, J. M.; Johnston, J. C. *J. Am. Chem. Soc.* **1978**, *100*, 4676.

(40) Kalyanasundaram, N.; Thomas, J. K. *J. Am. Chem. Soc*. **1977**, *99*, 2039.
(41) Nakajima, A. *J. Lumin.* **1977**, *15*, 277.
(42) Strickler, S. J.; Berg, R. A. *J. Chem. Phys.* **1962**, *37*, 814.
(43) Berlman, I. B. *Handbook of Fluorescence Spectra of Aromatic Molecules*, 2nd ed.; Academic Press: New York, 1971.
(44) Toma, R. P. D.; Brand, L. *Chem. Phys. Lett.* **1977**, *47*, 231.
(45) Sadkowski, P. J.; Fleming, G. R. *Chem. Phys.* **1980**, *54*, 79.
(46) Li, Y.-H.; Chan, L.-M.; Tyer, L.; Moody, R. T.; Himel, C. M.; Hercules, D. M. *J. Am. Chem. Soc.* **1975**, *97*, 3118.
(47) Mataga, N. *Bull. Chem. Soc. Jpn.* **1963**, *36*, 654.
(48) Bunton, C. A.; Minch, M. J.; Hidalgo, J.; Sepulveda, L. *J. Am. Chem. Soc.* **1973**, *95*, 3262.
(49) Garcia, M. E. D.; Sanz-Medel, A. *Talanta* **1986**, *33*, 255.
(50) Kinosita, K.; Kawato, S.; Ikegami, A. *Biophys. J*. **1977**, *20*, 289.
(51) Lipari, G.; Szabo, A. *Biophys. J.* **1980**, *30*, 489.
(52) Skomorokhov, V. I.; Dregalin, A. F. *Russ. J. Phys. Chem.* **1992**, *66*, 1569.
(53) Shinitzky, M.; Dianoux, A.-C.; Gitler, C.; Weber, G. *Biochemistry* **1971**, *10*, 2106.
(54) van Os, N. M.; Haak, J. R.; Rupert, L. A. M. *Physico-Chemical Properties of Selected Anionic, Cationic and Non-Ionic Surfactants*; Elsevier: Amsterdam, 1993.
(55) Berr, S.; Jones, R. R. M.; Johnson J. S., Jr. *J. Phys. Chem.* **1992**, *96*, 5611.
(56) Ishii, Y.; Matsuoka, H.; Ice, N. *Ber. Bunsen-Ges. Phys. Chem.* **1986**, *90*, 50.